Acta Crystallographica Section D
**Biological Crystallography**
ISSN 0907-4449

# Structural asymmetry of procaspase-7 bound to a specific inhibitor

**Hyo Jin Kang,[a,b]‡ Young-mi Lee,[b]‡ Kwang-Hee Bae,[c] Seung Jun Kim[c]* and Sang J. Chung[a,b]***

[a]Department of Chemistry, College of Natural Science, Dongguk University, 26 Pil-dong 3-ga, Jung-gu, Seoul 100-715, Republic of Korea, [b]BioNanotechnology Research Center, KRIBB, Yuseong, Daejeon 305-806, Republic of Korea, and [c]Systemic Proteomics Research Center, KRIBB, Yuseong, Daejeon 305-806, Republic of Korea

‡ These authors contributed equally to this work.

Correspondence e-mail: ksj@kribb.re.kr, sjchung@dongguk.edu

Received 16 November 2012
Accepted 14 April 2013

**PDB References:**
procaspase-7, 4hq0; complex with Ac-DEVD-CHO, 4hqr

Caspase-7 is expressed as a proenzyme and is activated by initiator caspases upon the transmission of cell-death signals. Despite extensive structural and biochemical analyses, many questions regarding the mechanism of caspase-7 activation remain unanswered. Caspase-7 is auto-activated during overexpression in *Escherichia coli*, even in the absence of initiator caspases, indicating that procaspase-7 has intrinsic catalytic activity. When variants of procaspase-7 with altered L2 loops were prepared, a variant with six inserted amino acids showed meaningful catalytic activity which was inhibited by Ac-DEVD-CHO. The kinetic constants of the procaspase-7 variant were determined and its three-dimensional structure was solved with and without bound inhibitor. The homodimeric procaspase-7 bound to the inhibitor revealed an asymmetry. One monomer formed a complete active site bound to the inhibitor in collaboration with the L2 loop from the other monomer, whereas the other monomer had an incomplete active site despite the bound inhibitor. Consequently, the two L2 loops in homodimeric procaspase-7 served as inherent L2 and L2′ loops forming one complete active site. These data represent the first three-dimensional structure of a procaspase-7 variant bound to a specific inhibitor, Ac-DEVD-CHO, and provide insight into the folding mechanism during caspase-7 activation and the basal activity level of procaspase-7.

## 1. Introduction

Apoptosis plays a key role in cell turnover, immune function, embryonic development, metamorphosis and chemical-dependent cell death; as a consequence, an imbalance in apoptotic regulation is involved in many human diseases (Soengas *et al.*, 2001; Taylor *et al.*, 2008). Excessively premature apoptosis may cause neurodegenerative diseases such as Alzheimer's, Parkinson's and Huntington's diseases, amyotrophic lateral sclerosis (ALS), multiple sclerosis (MS) or spinal muscular atrophy, whereas insufficient apoptotic death results in cancer (Mattson, 2000; Yuan & Yankner, 2000). Because caspase-7 is one of the final executioner proteins of apoptosis, regulation of its catalytic activity is of significant interest in the development of therapeutic strategies for both neurodegenerative diseases and cancers (Brown & Attardi, 2005; Feeney *et al.*, 2006; Letai, 2008; Mattson, 2000; Rotonda *et al.*, 1996).

Upon receiving death signals in mammalian cells, initiator caspases such as caspase-8, caspase-9 and caspase-10 activate procaspase-7 to mature caspase-7 by cleaving the inter-domain

**Table 1**
Constructs and corresponding primers for the preparation of procaspase-7 variants.

| Procaspase-7 variant | Plasmid | Forward primer† | Reverse primer† |
|---|---|---|---|
| Δ46 (Protein I) | P1 | 5′-GGGAATTC*CATATG*TCCATCAAGACCACCCG-GGA-3′ (F1) | 5′-CCG*CTCGAG*TTGACTGAAGTAGAGTTCCTT-GGT-3′ (R1) |
| Δ46/195TS-6aa (Protein II) | P2 | 5′-CTGGTGCCGCGCGGCAGCGCTAATCCTCGA-TAC-3′ (F2) | 5′-CTTGTATCGAGGATTAGCGCTGCCGCGCGG-CAC-3′ (R2) |
| Δ46/195TS (Protein III) | P3 | 5′-CTTGATGATGGC**CTGGTGCCGCGCGGCAGC**C-CCATCAATGACACA-3′ (F3) | 5′-GTCATTGATGGGGCTGCCGCGCGGCACCAGGCC-ATCATCAAG-3′ (R3) |
| Δ46/D198A/205TI (Protein IV) | P4 | 5′-GGGCCCATCAATGAC**CTGGTGCCGCGCGGC-AGC**ACAGATGCTAATCCTCGA-3′ (F4) | 5′-AGGATTAGCATCTGT**GCTGCCGCGCGGCACCA**-GGTCATTGATGGGCCCCGA-3′ (R4) |
| Δ46/D198A (Protein V) | P5 | 5′-GATGGCATCCAGGCC**GCG**TCGGGGCCCATC-AATGAC-3′ (F5) | 5′-GTCATTGATGGGCCCCGA**CGC**GGCCTGGATGCC-ATC-3′ (R5) |
| Δ46/C186S (Protein VI) | P6 | 5′-TTCTTCATTCAGGCT**TCT**CGAGGGACCGAG-CTTGAT-3′ (F6) | 5′-AAGCTCGGTCCCTCG**AGA**AGCCTGAATGAA-GAAGAG-3′ (R6) |
| Δ46/195TS-G6 (Protein VII) | P7 | 5′-GGCCTGGTGCCGCGCGGTAGC**GGCGGCGG-TGGCGGTGGC**GCTAATCCTCGATACAAG-ATC-3′ (F7) | 5′-GATCTTGTATCGAGGATTAGC**GCCACCGCCAC-CGCCGC***C*CGCTACCGCGCGGCACCAGGCC-3′ (R7) |
| Δ46/195TS-G3 (Protein VIII) | P8 | 5′-CCGCGCGGTAGCCCCATCAAT**GGCGGTGGC**-GCTAATCCTCGATACAAGATC-3′ (F8) | 5′-GATCTTGTATCGAGGATTAGC**GCCACCGCC**AT-TGATGGGGCTACCGCGCGG-3′ (R8) |

connector (IDC), the L2 loop, which connects the large and small subunits of procaspase-7 (Denault *et al.*, 2006; Boucher *et al.*, 2011). When overexpressed in *Escherichia coli*, however, procaspase-7 becomes a mature enzyme that is cleaved into small and large subunits even in the absence of initiator caspases (Denault & Salvesen, 2003; Stennicke & Salvesen, 1999; Zhou & Salvesen, 1997). This maturation of procaspase-7 was not observed in the catalytically inactive C186S procaspase-7 or D198A caspase-7 (Denault *et al.*, 2006; Boucher *et al.*, 2011). This finding indicates that wild-type procaspase-7 is self-activated through autocleavage at Asp198 during overexpression in *E. coli*. Because procaspase-7 is not activated until 2 h of overexpression in *E. coli* (Denault *et al.*, 2006; Boucher *et al.*, 2011), it is obvious that the protein can only be auto-activated at a high cellular concentration. To date, however, there has been no plausible explanation for this autocleavage process at a molecular level.

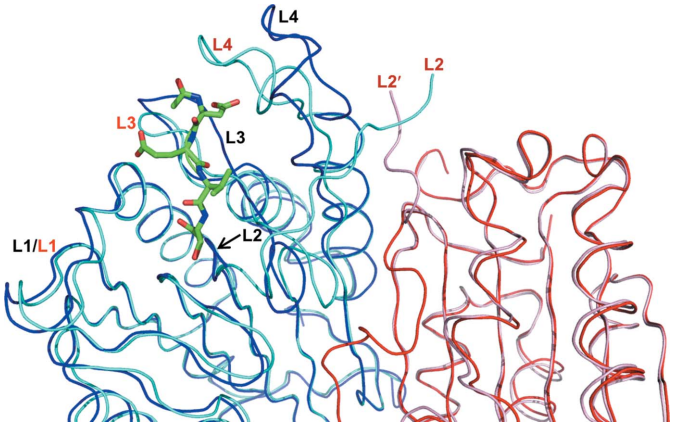


**Figure 1**
Structural superposition of mature caspase-7 bound to the inhibitor (cyan and pale pink) and procaspase-7 (blue and red) shown as worm models. The inhibitor (Ac-DEVD-CHO) bound to the active caspase-7 is shown as a stick model. The loops constituting the active site of the mature caspase-7 and procaspase-7 are labelled in black and red, respectively.

When an initiator caspase cleaves the inter-domain L2 loop of procaspase-7, the dimeric procaspase-7 converts each half of the homodimer into one large and one small subunit and undergoes dramatic conformational changes to form the active site (Fig. 1). The active site of caspase-7 consists of four loops, which were designated L1 (residues 76–87), L2 (residues 187–196), L3 (residues 226–238) and L4 (residues 274–288). In addition, the L2′ loop (residues 212′–217′) from the other subunit of the homodimer sits between the L2 and L4 loops and forms van der Waals contacts with these loops (Fig. 1). With the exception of the L1 loop, the loops undergo dramatic structural changes during maturation (Chai *et al.*, 2001). Structural comparison of procaspase-7 with mature caspase-7 in the presence or absence of inhibitor clearly shows the structural changes involved in caspase maturation. Although a large amount of structural and biochemical data related to the activation mechanism of procaspase-7 have been acquired (Bose & Clark, 2001; Chai *et al.*, 2001; Denault & Salvesen, 2002; Denault *et al.*, 2006; Pop *et al.*, 2001; Riedl *et al.*, 2001; Roy *et al.*, 2001; Zhou & Salvesen, 1997), several key questions remain unanswered. How does procaspase-7 achieve a basal level catalytic activity, as inferred from its auto-activation during overexpression in *E. coli*? Do intermediates exist during the activation of procaspase-7? If there are intermediates, what is the folding sequence after the inter-domain loop cleavage of procaspase-7?

During an extension of our previous work (Lee *et al.*, 2010), we found significant catalytic activity of *N*-Δ46-procaspase-7 variants that had six amino acids inserted or deleted in the L2 loop, which consequently prevents the protein from auto-activation during overexpression in *E. coli*. These mutations adjust the conformational strains imposed on the L2 loop and disturb the safety catch on the L2′ loop (Roy *et al.*, 2001); thus, biochemical and structural analyses were expected to provide molecular insight into the precise mechanism of procaspase-7 activation. We describe detailed structures of the procaspase-7 mutant with and without the specific inhibitor Ac-DEVD-CHO. Additional biochemical characterization and this

structural information provide comprehensive insight into the mechanism of the basal level activity and the maturation process of procaspase-7.

## 2. Materials and methods

### 2.1. Materials

Primer synthesis and DNA sequencing were performed by Bioneer (Daejeon, Korea) and Genotech (Daejeon, Korea), respectively. The primers used for PCR are listed in Table 1. The caspase-7 substrate and inhibitor, Ac-DEVD-*p*NA and Ac-DEVD-CHO, respectively, were purchased from Anaspec (Fremont, California, USA). Protein expression and cleavage were monitored by 15% SDS–PAGE analysis. Caspase activity was measured by monitoring the absorption change at 405 nm based on the release of *p*-nitroanilide from hydrolysis of the substrate Ac-DEVD-*p*NA using a DU 800 UV–Vis spectrophotometer (Beckman Coulter). The amino-acid sequences of the engineered proteins were numbered based on wild-type procaspase-7.

### 2.2. Preparation of overexpression vectors

The DNA of procaspase-7 with the N-terminal 46 amino acids deleted was prepared by PCR amplification using the caspase-7 gene as template DNA, a forward primer F1 with an *Nde*I site and a reverse primer R1 with an *Xho*I site. The resulting DNA and pET21a expression vector were digested with *Nde*I and *Xho*I, respectively, and ligated to generate the overexpression vector P1. The primers used in the corresponding plasmid construction are listed in Table 1.

Constructs P2–P8 were prepared using the QuikChange site-directed mutagenesis kit (Stratagene) according to the supplier's protocol. Briefly, 1 µl *PfuTurbo* polymerase (2.5 U µl$^{-1}$) was added to a mixture of an appropriate template plasmid (1 ng), primers (200 p*M* each; Table 1) and dNTPs (250 µ*M* each) in the reaction buffer supplied with the kit. After 17 cycles on a thermocycler (368 K for 1 min, 328 K for 30 s and 341 K for 12 min), the reaction was cooled to 277 K and *Dpn*I (1 µl at 10 U µl$^{-1}$; New England Biolabs) was added to digest the parental DNA and hemimethylated plasmid. PCR products were transformed into XL-10 Gold cells (Invitrogen). Individual colonies were picked and grown for DNA amplification and the resultant plasmids were sequenced. Constructs P3, P5 and P6 were prepared from the P1 background, constructs P2, P7 and P8 were prepared from the P3 background and construct P4 was prepared from the P5 background.

### 2.3. Protein expression and purification

*E. coli* BL21 Rosetta cells (Novagen) carrying the respective vectors were grown at 310 K in LB medium until the optical density at $A_{600}$ reached 0.6–0.8. Expression of the engineered caspase-7 precursors was induced by adding 1 m*M* IPTG at 291 K for 18 h. The cells were harvested, washed with buffer *A* (50 m*M* Tris pH 7.5, 250 m*M* NaCl, 5% glycerol, 0.05% $\beta$-mercaptoethanol) and lysed by ultrasonication. After centrifugation (29 820*g* for 30 min at 277 K), the supernatant was incubated with cobalt-affinity resin (TALON, Clontech) on a rocker for 1 h at 277 K and washed with buffer *A* containing 10 m*M* imidazole. The protein was eluted from the metal-affinity resin using buffer *A* supplemented with 100 m*M* imidazole. After dialysis against 20 m*M* Tris pH 8.0, 10 m*M* NaCl, 1.25% glycerol, 1 m*M* dithiothreitol (DTT), the protein was purified using Mono Q ion-exchange column chromatography and was further purified on a Sephacryl S-100 size-exclusion column (Amersham Pharmacia) by elution with 20 m*M* HEPES pH 7.5, 100 m*M* NaCl, 2 m*M* DTT and concentrated to 20–25 mg ml$^{-1}$ for crystallization.

**Table 2**
Summary of statistics of data collection and refinement.

Values in parentheses are for the highest resolution shell.

| | Procaspase-7 (free Protein IV) | Procaspase-7–Ac-DEVD-CHO (Protein IV–Ac-DEVD-CHO) |
|---|---|---|
| Data collection | | |
| Resolution (Å) | 40–3.0 (3.16–3.00) | 40–3.0 (3.16–3.00) |
| Space group | $P3_221$ | $P3_221$ |
| Unit-cell parameters (Å, °) | $a = b = 89.60$, $c = 182.84$, $\alpha = \beta = 90$, $\gamma = 120$ | $a = b = 90.48$, $c = 185.05$, $\alpha = \beta = 90$, $\gamma = 120$ |
| Total reflections | 183564 | 183096 |
| Unique reflections | 17689 | 18228 |
| Completeness (%) | 100 (100) | 100 (100) |
| Multiplicity | 10.4 (10.8) | 10.0 (10.2) |
| $\langle I/\sigma(I)\rangle$ | 7.3 (1.6) | 8.0 (1.9) |
| $R_{\rm merge}$† (%) | 8.8 (47.3) | 8.5 (40.5) |
| Refinement | | |
| No. of reflections | 17639 | 18188 |
| No. of atoms | 3428 | 3653 |
| $R_{\rm work}/R_{\rm free}$ (%) | 22.2/26.7 | 21.8/25.3 |
| R.m.s. deviations from ideal geometry | | |
| Bond distances (Å) | 0.008 | 0.008 |
| Bond angles (°) | 1.38 | 1.38 |
| Dihedral angles (°) | 23.75 | 24.75 |
| Improper angles (°) | 0.92 | 0.79 |
| Average *B* factor (Å$^2$) | 68.91 | 57.12 |

† $R_{\rm merge} = \sum_{hkl}\sum_i |I_i(hkl) - \langle I(hkl)\rangle| / \sum_{hkl}\sum_i I_i(hkl)$, where $I_i(hkl)$ is the intensity of the *i*th measurement of an equivalent reflection with indices *hkl*.

### 2.4. Kinetic analysis of procaspase-7 variants

The catalytic activity of each enzyme was measured using the colorimetric caspase substrate Ac-DEVD-*p*NA. Briefly, procaspase-7 enzyme activity was measured in reaction buffer (50 m*M* HEPES pH 7.4, 50 m*M* KCl, 2 m*M* $MgCl_2$, 1 m*M* EDTA, 5 m*M* DTT) at room temperature (RT). An appropriate amount of a caspase-7 precursor or an activated caspase-7 (final concentrations of 10–300 n*M*) was added to various concentrations of substrate solution (0, 15, 30, 60, 120, 240 and 480 µ*M*). The *p*-nitroanilide released by the caspase reaction was monitored at 405 nm using a DU 800 UV–Vis spectrophotometer (Beckman Coulter) or a VICTOR X2 plate reader (PerkinElmer). The $K_{\rm m}$ and $V_{\rm max}$ values were calculated using *Hyper*32 v.1.0.0 (http://homepage.ntlworld.com/john.easterby/hyper32.html) and the $k_{\rm cat}$ values were calculated from the $V_{\rm max}$ and the enzyme concentration used.

**Table 3**
Kinetic parameters of procaspase-7 variants for hydrolysis of Ac-DEVD-*p*NA.

ND, not determined.

| Procaspase-7 variant | $K_m$ ($\mu M$) | $k_{cat}$ ($min^{-1}$) | $k_{cat}/K_m$ ($M^{-1}$ $min^{-1}$) |
|---|---|---|---|
| Δ46 (Protein I) | 116.4 ± 4.2 | 461.6 ± 2.0 | (4.0 ± 0.0) × $10^6$ |
| Δ46/195TS-6aa (Protein II) | 109.6 ± 3.4 | 1.1 ± 0.0 | (1.0 ± 0.0) × $10^4$ |
| Δ46/195TS (Protein III) | ND | ND | ND |
| Δ46/D198A/205TI (Protein IV) | 82.7 ± 0.6 | 2.7 ± 0.1 | (3.0 ± 0.0) × $10^4$ |
| Protein II + thrombin | 437.6 ± 2.8 | 66.0 ± 0.3 | (1.5 ± 0.0) × $10^5$ |
| Protein III + thrombin | 611.9 ± 10.9 | 61.9 ± 1.0 | (1.0 ± 0.0) × $10^5$ |
| Protein IV + thrombin | 151.6 ± 6.8 | 290.8 ± 9.2 | (1.9 ± 0.0) × $10^6$ |
| Δ46/195TS-G6 (Protein VII) | 123.9 ± 11.8 | 1.64 ± 0.0 | (1.3 ± 0.0) × $10^4$ |
| Δ46/195TS-G3 (Protein VIII) | 114.1 ± 3.4 | 2.37 ± 0.0 | (2.1 ± 0.0) × $10^4$ |

### 2.5. Crystallization of Δ46/D198A/205TI procaspase-7 (Protein IV) in the presence and absence of the inhibitor, X-ray data collection and structure determination

A stock solution of Protein IV was prepared at a final concentration of 25 mg $ml^{-1}$ in 20 m*M* HEPES pH 7.5, 100 m*M* NaCl, 2 m*M* DTT. Crystals of Protein IV were grown by mixing 1 µl Protein IV stock solution and an equal volume of reservoir solution (100 m*M* sodium acetate pH 4.6, 2 *M* sodium formate) at RT. After 3 d, Protein IV crystals grew to their full dimensions. The crystals diffracted to 3.0 Å resolution and belonged to space group $P3_221$, with unit-cell parameters $a = b = 89.60$, $c = 182.84$ Å, $\alpha = \beta = 90$, $\gamma = 120°$. To prepare crystals of Protein IV bound to Ac-DEVD-CHO, the protein stock solution was mixed with ten equivalents of Ac-DEVD-CHO. The resulting mixture was concentrated to a final concentration of 25 mg $ml^{-1}$ and then incubated at RT for 2 h. The protein–inhibitor complex (1 µl) was mixed with an equal volume of reservoir solution (100 m*M* sodium acetate pH 4.6, 2 *M* sodium formate). Crystals grew within 3 d at RT. The crystals diffracted to 3.0 Å resolution and belonged to space group $P3_221$, with unit-cell parameters $a = b = 90.48$, $c = 185.05$ Å, $\alpha = \beta = 90$, $\gamma = 120°$. All diffraction data were collected on beamline 6C at the Pohang Accelerator Laboratory, Pohang, Republic of Korea using an ADSC Quantum 4 detector. The diffraction data collected were processed and scaled with *MOSFLM* (Leslie, 1999) and *SCALA* (Winn *et al.*, 2011). The statistics of data collection and refinement are shown in Table 2. The atomic coordinates and structural parameters of the final structures of free and Ac-DEVD-CHO-bound procaspase-7 (Protein IV) have been deposited in the PDB as entries 4hq0 and 4hqr, respectively.

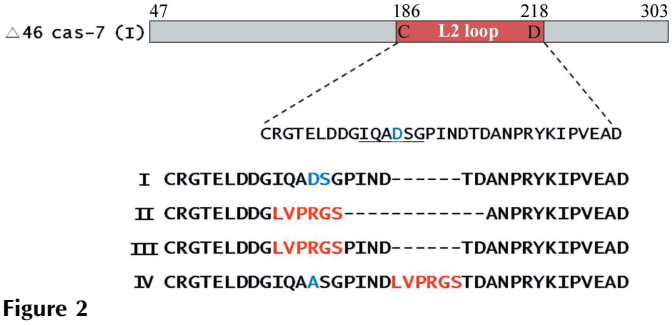


**Figure 2**
Sequence alignment of procaspase-7 variants. I, procaspase-7 devoid of the N-terminal 46 amino acids (Δ46 procaspase-7); II, amino acids 195–200 of Δ46 procaspase-7 were replaced with LVPRGS (a sequence susceptible to thrombin) with the additional deletion of PINDT from the L2 loop; III, amino acids 195–200 of Δ46 procaspase-7 were replaced by LVPRGS; IV, an additional LVPRGS motif was inserted between Asp204 and Thr205 of Δ46 procaspase-7 and Asp198 was mutated to Ala.

## 3. Results and discussion

### 3.1. Preparation of procaspase-7 variants

A series of procaspase-7 variants with L2 loops of various lengths were designed and prepared to explore the effect of the strain imposed on the L2 loop on the intrinsic activity of procaspase-7 (Fig. 2). Because the N-terminal prodomain of procaspase-7 is known to be dispensable for caspase-7 activity, the DNA corresponding to the N-terminal 46 amino acids was removed from the full-length procaspase-7 gene. The residual DNA was inserted into plasmid DNA, resulting in plasmid P1 for N-Δ46 procaspase-7 (Protein I) overexpression. From the P1 background, four further constructs were prepared that contained an insertion of six amino acids, LVPRGS, corresponding to a thrombin-substrate sequence in which thrombin cleaves the peptide bond between R and G, into the L2 loop as a latent activation site (Fig. 2; Lee *et al.*, 2010). Proteins II and III have a substitution in which LVPRGS replaces six amino acids ($I^{195}$QADSG$^{200}$; Fig. 1). Protein IV was prepared by inserting LVPRGS between Asp204 and Thr205 into the L2 loop with a D198A mutation. Protein II has an L2 loop that is six amino acids (PINDTD) shorter than that of wild-type procaspase-7.

While Protein I purified as large and small subunits as usual, Proteins II–IV were overexpressed and purified as single

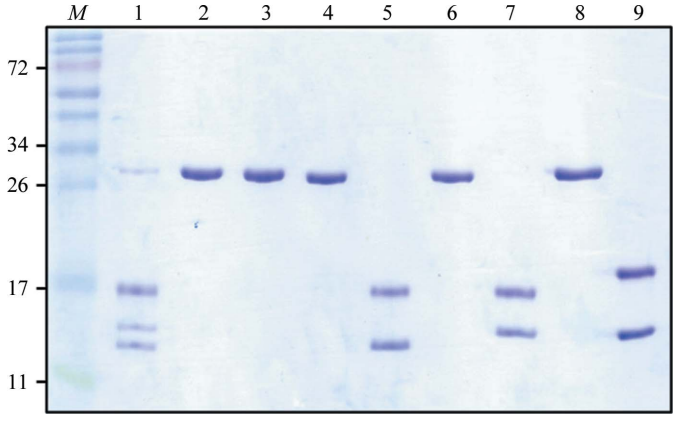


**Figure 3**
Activation of caspase-7 precursors by thrombin digestion. SDS–PAGE analysis of procaspase-7 variants. Procaspase-7 variants were treated with thrombin at 277 K for 18 h. Lane *M*, molecular-mass size marker (labelled in kDa); lane 1, Protein I (Δ46 caspase-7); lane 2, C186S Δ46 procaspase-7; lane 3, Δ46/D198A procaspase-7; lane 4, Protein II (Δ46/195TS-6aa procaspase-7); lane 5, Δ46/195TS-6aa procaspase-7 (Protein II) processed with thrombin; lane 6, Protein III (Δ46/195TS procaspase-7); lane 7, Δ46/198TS procaspase-7 (Protein III) processed with thrombin; lane 8, Protein IV (Δ46/D198A/205TI procaspase-7); lane 9, Δ46/D198A/205TI procaspase-7 (Protein IV) processed with thrombin.

polypeptides. Proteins II–IV were cleaved into large and small subunits by thrombin digestion (Fig. 3).

### 3.2. Kinetic analysis of the procaspase-7 variants

The catalytic activities of the procaspase-7 variants were analyzed using Ac-DEVD-*p*NA, a representative colorimetric substrate (Datta *et al.*, 1996). The kinetic parameters thus obtained are listed in Table 3. Interestingly, Proteins II and IV, which resemble the procaspase-7 zymogen, showed significant catalytic activity. This finding differs from the previous report (Boucher *et al.*, 2011). The kinetic constants for the hydrolysis of Ac-DEVD-*p*NA were determined for three of the four procaspase-7 zymogen analogues, but we were unable to determine the kinetic constants for Δ46/195TS procaspase-7 (Protein III) owing to its low catalytic activity. Detailed inspection of the kinetic constants revealed a more interesting feature, which is that the $K_m$ values of the zymogen analogues are smaller than that of wild-type caspase-7 (Table 3). This observation differs from the previous suggestion that the L2 loop cleavage is essential for caspase-7 to form an active site capable of substrate binding (Denault *et al.*, 2006; Riedl *et al.*, 2001; Chai *et al.*, 2001). However, the observed results explain the self-activation property of procaspase-7. As the length of the L2 loop increased, the turnover number ($k_{cat}$) of Δ46/D198A/205TI procaspase-7 (Protein IV) increased over that of Δ46/195TS procaspase-7 (Protein III). This result is in agreement with the previous report that the strain imposed on the L2 loop prevents the catalytic cysteine from rotating into the active orientation (Chai *et al.*, 2001; Kang *et al.*, 2012). In this regard, it is interesting that Δ46/195TS-6aa procaspase-7 (Protein II) had measurable catalytic activity ($k_{cat}/K_m$ = $1.0 \times 10^4\ M^{-1}\ s^{-1}$) but Δ46/195TS procaspase-7 (Protein III) did not show sufficient activity to determine the kinetic constants. To test whether alternatively cleaved proteins from Proteins II and IV showed catalytic activity, we performed Western blot analysis of Proteins II, III and IV (Supplementary Fig. S1[1]). However, none of the proteins showed a cleaved protein.

The catalytic activity observed for Protein II was not consistent with the strain hypothesis described above. We noted that Protein II lacks the amino acids $P^{201}$INDTD$^{206}$ on the L2 loop. Among these six amino acids, the three amino acids DTD correspond to the 'DDD safety catch' region in caspase-3 that maintains procaspase-3 in an inactive conformation (Roy *et al.*, 2001). Therefore, we mutated the six amino acids $P^{201}$INDTD$^{206}$ in Protein III, resulting in Proteins VII (all six amino acids were mutated to six glycine residues) and VIII (the three amino acids DTD were mutated to three glycine residues; Table 1). Proteins VII and VIII showed significant catalytic activities that were comparable to those of Proteins II and IV (Table 3). These data demonstrate that the catalytic activity of Protein II arose from disturbance of the safety-catch region. This may also be true for the catalytic activity observed in Protein IV. In addition, the substrate specificity of the procaspase-7 mutants increased as the length of the L2 loop increased, suggesting that the strain imposed on the L2 loop is also involved in regulating the catalytic activity of procaspase-7.

When Proteins II–IV were treated with thrombin, they were all completely cleaved into large and small subunits. The substrate specificity ($k_{cat}/K_m$) of Protein IV for Ac-DEVD-*p*NA hydrolysis increased from $3.0 \times 10^4$ to $1.9 \times 10^6\ M^{-1}\ s^{-1}$, a 63-fold increase, after thrombin digestion. Proteins II and III showed a more than tenfold increase in substrate specificity ($k_{cat}/K_m$) for Ac-DEVD-*p*NA when the L2 loop was cleaved with thrombin. The catalytic activity of all of the procaspase-7 variants was inhibited by a specific caspase-7 inhibitor, Ac-DEVD-CHO, in a concentration-dependent manner (data not shown). Interestingly, the $K_m$ values of Proteins II and IV for Ac-DEVD-*p*NA were determined to be 109.6 and 82.7 μ*M*, respectively, which are similar to that of wild-type caspase-7 (116.4 μ*M*). In contrast, their $k_{cat}$ values were determined to be 1.1 and 2.7 $min^{-1}$, respectively, which were at least 60-fold lower than those of the corresponding thrombin-treated enzymes. This indicates that the poor substrate specificity resulted primarily from low turnover number ($k_{cat}$) rather than low binding affinity ($K_m$). Although the low $K_m$ values may be partially influenced by the low $k_{cat}$, such strong binding of the substrate is very surprising because previous structural data for procaspase-7 revealed an incomplete active site owing

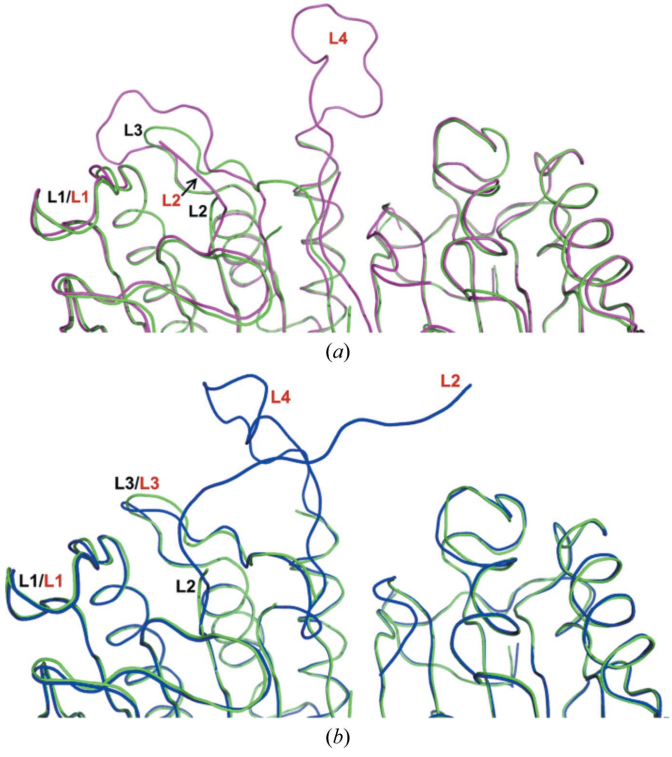


**Figure 4**
Structural comparison of free Protein IV (green) with procaspase-7 (PDB entry 1k88; magenta) (*a*) and free mature caspase-7 (PDB entry 1k86; blue) (*b*). The point of view in (*a*) is the same as in (*b*). The loops constituting the active site are labelled in black (free Protein IV) and red (the counterpart).

[1] Supplementary material has been deposited in the IUCr electronic archive (Reference: MH5082). Services for accessing this material are described at the back of the journal.

to inappropriate L2 and L4 loop formation compared with mature caspase-7 (Chai *et al.*, 2001). The kinetic data suggest that the substrate binding of procaspase-7 is as efficient as that of the mature caspase-7 but that its catalysis is not.

The current results may explain the origin of the basal level of activity of procaspase-7 that is responsible for autocleavage during overexpression. However, it remained unknown how the procaspase-7 zymogen analogues were able to catalyze the reaction when unable to correctly form the active site because the lack of cleavage of the L2 loop prohibited the essential loop rearrangement. To answer this question, we crystallized Protein IV in the presence and absence of Ac-DEVD-CHO and determined the structure of inhibitor-bound and free Protein IV. SDS–PAGE analysis confirmed that the protein in the crystals was a single polypeptide (Supplementary Fig. S2).

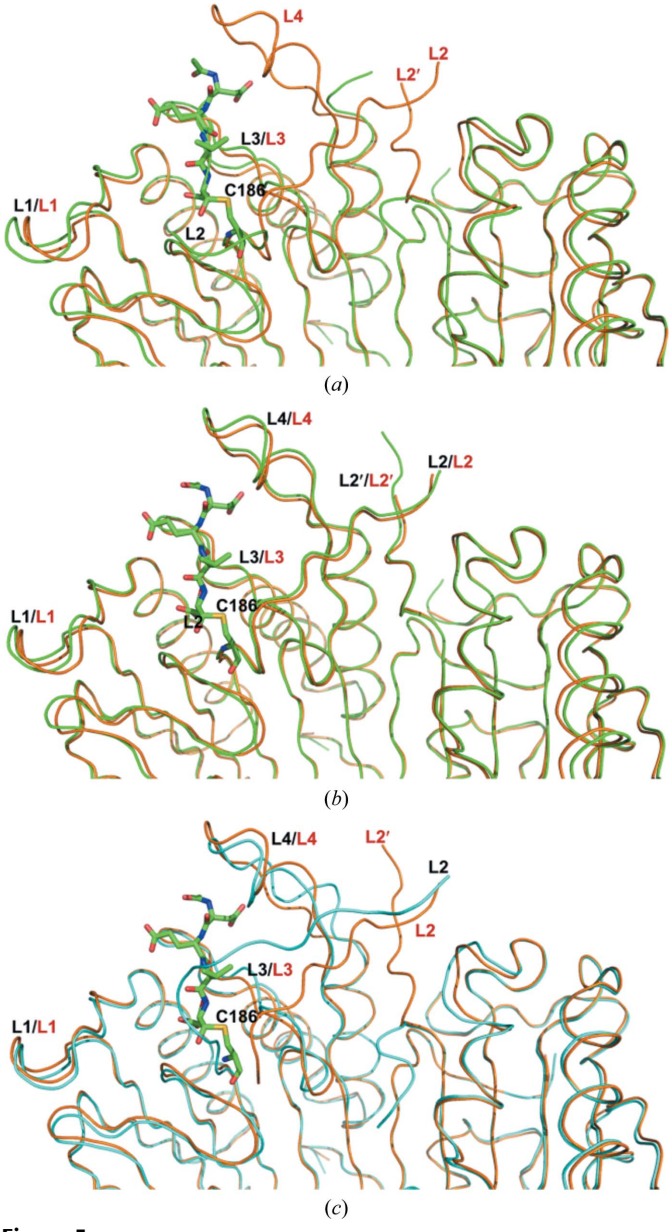


**Figure 5**
Structural superposition of mature caspase-7 in complex with Ac-DEVD-CHO (PDB entry 1f1j; orange) with partially active Protein IV bound to Ac-DEVD-CHO (green) (*a*) and with fully active Protein IV bound to Ac-DEVD-CHO (green) (*b*). Only the inhibitor Ac-DEVD-CHO bound to Protein IV is shown in the drawing for clarity. The loops constituting the active site are labelled in black (Protein IV) and red (the counterpart). (*c*) Structural superposition of fully active Protein IV bound to Ac-DEVD-CHO (orange and labelled in red) with free mature caspase-7 (PDB entry 1k86; cyan and labelled in black).

### 3.3. Structure of free Δ46/D198A/205TI procaspase-7 (Protein IV)

The crystal structures of free and Ac-DEVD-CHO-bound Δ46/D198A/205TI procaspase-7 (Protein IV) were determined using the structure of native caspase-7 (PDB entry 1k86; Chai *et al.*, 2001) as a starting model. The final $R_{\rm cryst}$ and $R_{\rm free}$ values were 22.2 and 26.7%, respectively, for free Δ46/D198A/205TI procaspase-7 (Protein IV) and 21.8 and 25.3%, respectively, for Ac-DEVD-CHO-bound Δ46/D198A/205TI procaspase-7 (Protein IV). Overall, the geometry and the electron-density map were of good quality. The models were validated using the program *PROCHECK*. A Ramachandran plot drawn by *PROCHECK* showed that 98.1 and 99.5% of the residues in the free and the inhibitor-bound Δ46/D198A/205TI procaspase-7 (Protein IV) models, respectively, fall within the most favoured or additional allowed regions.

Overall, the structure of the free Protein IV dimer showed good alignment with either procaspase-7 (PDB entry 1k88; r.m.s. deviation of 0.57 Å for 402 $C^{\alpha}$ atoms of the dimer; Chai *et al.*, 2001) or mature caspase-7 (PDB entry 1k86; r.m.s. deviation of 0.54 Å for 407 $C^{\alpha}$ atoms of the dimer). However, the loops that constitute the active site adopted different conformations compared with either mature caspase-7 or procaspase-7. In particular, the L3 loop in free Protein IV (residues 225–239) was in the active conformation in the dimer even in the uncleaved state (Fig. 4). Although residues 226–227 in one protomer and residues 227–230 in the other protomer are disordered, the remaining part of the L3 loop in free Protein IV has an active conformation similar to that of mature caspase-7.

In contrast, residues 228–239 of the structures of mature caspase-7 and free Protein IV with a partially active conformation can be superposed. We speculated that extending the L2 loop by six residues would enable the L3 loop to adopt an active conformation. The other noticeable change occurred in the L4 loop. Residues 275–285 in the L4 loop of free Protein IV are disordered, whereas the corresponding residues of the proenzyme are ordered but without contacts with the active-site loops and body of procaspase-7. This loop appeared to be important and it appears that the conformational change in the L3 loop is the initial activation step because residues 229–230 of procaspase-7 overlapped with the covalently linked inhibitor in the mature caspase-7 model.

### 3.4. Structure of Δ46/D198A/205TI procaspase-7 (Protein IV) bound to Ac-DEVD-CHO

The structure of Protein IV bound to Ac-DEVD-CHO showed an asymmetry in the active-site loop conformation within the dimer. One protomer of the dimer adopted a

partially active conformation and had a very similar structure to that of free Protein IV; both have the same L3 loop conformation. However, the L2 loop at the N-terminus is extended and inserted between the L3 loop and strand 3a, which allows the catalytic Cys186 of the L2 loop to adopt a productive conformation (Fig. 5*a*). The remaining loops (L2′, L2 at the C-terminus and L4) are unchanged compared with the free Protein IV model. This structural feature reminded us of the engineered hybrid dimer reported by Salvesen and coworkers (Denault *et al.*, 2006). They showed that a caspase-7 dimer consisting of one active monomer and a procaspase-7 monomer showed nearly the same catalytic activity as wild-type caspase-7. Although the loops that constitute the active site are not fully engaged in the active conformation, the covalent linkage between Protein IV and Ac-DEVD-CHO may be formed by the productive conformation of the catalytic Cys186 and the lengthy crystallization process. In addition, the high reactivity of the aldehyde of the inhibitor with a nucleophile would facilitate the formation of a covalent bond to Cys186. The average value of the thermal factors for the Ac-DEVD-CHO inhibitor bound to one protomer is 91.3 Å$^2$ (compared with 61.0 Å$^2$ for the rest of the protomer), while that for the Ac-DEVD-CHO inhibitor of the other protomer of the same dimer is 60.5 Å$^2$ (compared with 51.0 Å$^2$ for the rest of the protomer), suggesting that Ac-DEVD-CHO is not fully occupied in the former protomer.

In the other protomer of the dimer, Ac-DEVD-CHO-bound Protein IV adopts a fully active conformation in response to Ac-DEVD-CHO binding. All of the active-site loops (L1, L2, L2′, L3 and L4) are nearly completely superposed with those of mature caspase-7 in complex with Ac-DEVD-CHO (PDB entry 1f1j; Wei *et al.*, 2000; r.m.s. deviation of 0.36 Å for 227 C$^\alpha$ atoms of the protomer; Fig. 5*b*). The catalytic Cys186 in the L2 loop is also covalently linked to its inhibitor, retaining the productive conformation. These crystallographic observations are consistent with the kinetic data showing that Protein IV has intrinsic catalytic activity towards Ac-DEVD-*p*NA.

To confirm the number of active sites in Protein IV, we measured the enzyme activity in the presence of Ac-DEVD-CHO at a series of concentrations (Supplementary Fig. S3). When 100 n*M* Protein IV was used, the IC$_{50}$ for enzyme inhibition by Ac-DEVD-CHO was determined to be 26 n*M*. If each enzyme molecule forms one active site, the IC$_{50}$ value would be expected to be 50 n*M*. However, the observed IC$_{50}$ was roughly half of the expected value, meaning that only half of the used enzyme was active. Considering that the enzyme acts as a dimer, only one monomer of the dimer was expected to have an active conformation. This observation is consistent with the active-site structure of Protein IV bound to Ac-DEVD-CHO in that one monomer of the dimer has a fully active conformation while the other does not.

According to a previous report (Chai *et al.*, 2001), active caspase-7 without an inhibitor bound at the active site does not have a well defined catalytic site or loop bundle, whereas complete formation of the loop bundle of caspase-7 is accompanied by substrate or inhibitor binding. The current observations, together with the previous report, therefore imply that the structural differences observed between procaspase-7 and active caspase-7 bound to the inhibitor primarily result from induced-fit binding of the inhibitor. In contrast, the asymmetric feature found in the inhibitor-bound Protein IV structure may result from the strain imposed on the L2 loop. For caspase-7 to form an active conformation, the L2 loop from one monomer should interact with the L2′ loop from the other monomer. Because they are separated in each monomer of mature caspase-7, the L2 and L2′ loops can independently associate with the L2 and L2′ loops from the other monomer. As a result, the enzyme can form two active sites with Cys186 in a productive orientation. In procaspase-7, however, the L2 and L2′ loops are covalently connected with a

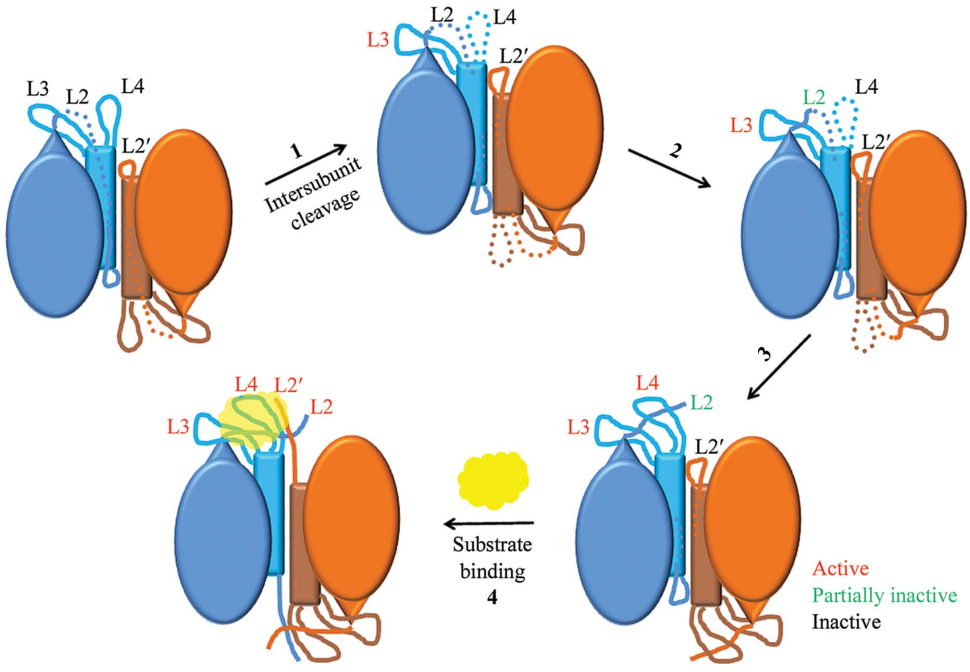


**Figure 6**
The activation model of caspase-7 is shown in the following four steps. Step 1: Upon cleavage of inter-domain L2 loop, the L3 loop rearranges to an optimal conformation for catalysis, while the L4 loop is disordered. Step 2: The N-terminus of the L2 loop adopts a catalytically productive conformation. Step 3: The L4 and L2 loops at the C-terminus are changed to the active conformation. Step 4: Substrate binding induces a drastic conformational change of the L2′ loop of the other protomer, completing the fully active conformation.

limited length. Consequently, the L2 loop of one monomer can only take the role of the L2 or L2′ loop, whereas the L2 loop of the other monomer can take the complementary role, resulting in only one active site with Cys186 in a productive orientation. However, the low $k_{cat}$ of Protein IV indicates that the orientation of Cys186 may not be sufficient for catalysis compared with its orientation in mature caspase-7.

The current structural observations, together with the kinetic data, suggest that procaspase-7 can form at least one complete active site in the dimer to accommodate substrate binding, which is sufficient for full catalytic power (Denault *et al.*, 2006). Therefore, control of the catalytic activity by the L2 loop is mainly achieved through controlling the orientation of the catalytic Cys186 rather than through active-site formation.

Based on the crystallographic observations and biochemical characterization, the activation process for caspase-7 can be viewed as four modes of operation (Fig. 6). In the initial step, cleavage of the inter-subunit linker (L2) allows the L3 loop to be stabilized in the active conformation, while the L4 loop is disordered. The disorder of the L4 loop of procaspase-7 is important because this can make room for the L2 and L2′ loops to be positioned in the active conformation later. The L2 loop at the N-terminus can be oriented in the productive conformation for substrate or inhibitor binding. Based on the active caspase-7 structure in the apo state (PDB entry 1k86), the L4 loop adopts the active conformation. At the same time, the L2 loop changes direction to extend away from the dimer body. Upon substrate or inhibitor binding, the L2 loop moves towards the L4 loop of the same protomer and the L2′ loop from the other protomer flips and stretches between the L2 and L4 loops, completing the activation by stabilizing the loop bundle formed.

## 4. Conclusion

The L2 loop of procaspase-7 was mutated to prohibit auto-activation in the *E. coli* expression system, but it could be activated by limited thrombin digestion. A procaspase variant with six amino acids inserted (Δ46/D198A/205TI procaspase-7; Protein IV) showed meaningful catalytic activity, with a $K_m$ of 82.7 μ*M* for hydrolysis of Ac-DEVD-*p*NA, and its activity was specifically inhibited by Ac-DEVD-CHO. Interestingly, the binding affinity of Protein IV for the substrate was similar to that of wild-type mature caspase-7 or its corresponding mature form. Protein IV was crystallized in the presence or absence of the inhibitor Ac-DEVD-CHO, resulting in three-dimensional structures of free and inhibitor-bound Protein IV. The inhibitor-bound Protein IV homodimer revealed an asymmetric structure in which one monomer has a fully mature structure similar to that of mature caspase-7 bound to Ac-DEVD-CHO but the other has a partially mature structure. In detail, the L2 loop in one protomer acted as the L2 loop in mature caspase-7, whereas the L2 loop in the other protomer played the role of the L2′ loop, resulting in only one active site with Cys186 in a productive orientation. In addition, an active-site titration of Protein IV with Ac-DEVD-CHO demonstrated that half of the protein IV used is active. To the best of our knowledge this is the first structure of procaspase-7 bound to a specific inhibitor and may provide answers to many questions regarding the activation mechanism and the origin of the basal level of activity of procaspase-7.

This work was supported by National Research Foundation of Korea (NRF) grants (Nos. 2006-2005077, 2010-0019926, 2012M3A9C4048775 and 2012-0009543) funded by the Korea government (MEST) and the Dongguk University Research Fund of 2013.

## References

Bose, K. & Clark, A. C. (2001). *Biochemistry*, **40**, 14236–14242.
Boucher, D., Blais, V., Drag, M. & Denault, J.-B. (2011). *Biosci. Rep.* **31**, 283–294.
Brown, J. M. & Attardi, L. D. (2005). *Nature Rev. Cancer*, **5**, 231–237.
Chai, J., Wu, Q., Shiozaki, E., Srinivasula, S. M., Alnemri, E. S. & Shi, Y. (2001). *Cell*, **107**, 399–407.
Datta, R., Banach, D., Kojima, H., Talanian, R. V., Alnemri, E. S., Wong, W. W. & Kufe, D. W. (1996). *Blood*, **88**, 1936–1943.
Denault, J.-B., Békés, M., Scott, F. L., Sexton, K. M., Bogyo, M. & Salvesen, G. S. (2006). *Mol. Cell*, **23**, 523–533.
Denault, J.-B. & Salvesen, G. S. (2002). *Chem. Rev.* **102**, 4489–4500.
Denault, J.-B. & Salvesen, G. S. (2003). *J. Biol. Chem.* **278**, 34042–34050.
Feeney, B., Pop, C., Swartz, P., Mattos, C. & Clark, A. C. (2006). *Biochemistry*, **45**, 13249–13263.
Finney, D. J. (1983). *Clin. Chem.* **29**, 1762–1766.
Kang, H. J., Lee, Y.-M., Jeong, M. S., Kim, M., Bae, K.-H., Kim, S. J. & Chung, S. J. (2012). *Biosci. Rep.* **32**, 305–313.
Lee, Y.-M., Kang, H. J., Jang, M., Kim, M., Bae, K.-H. & Chung, S. J. (2010). *Protein Expr. Purif.* **69**, 29–33.
Leslie, A. G. W. (1999). *Acta Cryst.* D**55**, 1696–1702.
Letai, A. G. (2008). *Nature Rev. Cancer*, **8**, 121–132.
Mattson, M. P. (2000). *Nature Rev. Mol. Cell Biol.* **1**, 120–129.
Pop, C., Chen, Y.-R., Smith, B., Bose, K., Bobay, B., Tripathy, A., Franzen, S. & Clark, A. C. (2001). *Biochemistry*, **40**, 14224–14235.
Riedl, S. J., Fuentes-Prior, P., Renatus, M., Kairies, N., Krapp, S., Huber, R., Salvesen, G. S. & Bode, W. (2001). *Proc. Natl Acad. Sci. USA*, **98**, 14790–14795.
Rotonda, J., Nicholson, D. W., Fazil, K. M., Gallant, M., Gareau, Y., Labelle, M., Peterson, E. P., Rasper, D. M., Ruel, R., Vaillancourt, J. P., Thornberry, N. A. & Becker, J. W. (1996). *Nature Struct. Biol.* **3**, 619–625.
Roy, S., Bayly, C. I., Gareau, Y., Houtzager, V. M., Kargman, S., Keen, S. L., Rowland, K., Seiden, I. M., Thornberry, N. A. & Nicholson, D. W. (2001). *Proc. Natl Acad. Sci. USA*, **98**, 6132–6137.
Soengas, M. S., Capodieci, P., Polsky, D., Mora, J., Esteller, M., Opitz-Araya, X., McCombie, R., Herman, J. G., Gerald, W. L., Lazebnik, Y. A., Cordón-Cardó, C. & Lowe, S. W. (2001). *Nature (London)*, **409**, 207–211.
Stennicke, H. R. & Salvesen, G. S. (1999). *Methods*, **17**, 313–319.
Taylor, R. C., Cullen, S. P. & Martin, S. J. (2008). *Nature Rev. Mol. Cell Biol.* **9**, 231–241.
Wei, Y., Fox, T., Chambers, S. P., Sintchak, J., Coll, J. T., Golec, J. M. C., Swenson, L., Wilson, K. P. & Charifson, P. S. (2000). *Chem. Biol.* **7**, 423–432.
Winn, M. D. *et al.* (2011). *Acta Cryst.* D**67**, 235–242.
Yuan, J. & Yankner, B. A. (2000). *Nature (London)*, **407**, 802–809.
Zhou, Q. & Salvesen, G. S. (1997). *Biochem. J.* **324**, 361–364.